



In vitro anthelmintic activity and *in silico* analysis of monoterpenes, sesquiterpenes, and semisynthetic derivatives against *Eisenia foetida*

Andrea Leticia Cáceres^{1†} , Elvio Gayoso^{2†} , Rosa Guillen³ , Nelson Luis Alvarenga^{1*} 

¹Phytochemistry Department, Faculty of Chemical Sciences, National University of Asunción, San Lorenzo, Paraguay.

²Biology Department, Faculty of Exact and Natural Sciences, National University of Asunción, San Lorenzo, Paraguay.

³Microbiology Department, Institute of Health Sciences Research, National University of Asunción, San Lorenzo, Paraguay.

ARTICLE HISTORY

Received on: 29/06/2024

Accepted on: 14/10/2024

Available Online: 25/11/2024

Key words:

Anthelmintics, monoterpenes, sesquiterpenes, *in silico*, *Eisenia foetida*.

ABSTRACT

Helminthiasis remains a worldwide public health problem, mainly in not-developed countries. Available drugs are scarce, and the risk of developing resistance by the parasites is always present. Natural products remain a valid alternative in the search for new antiparasitic drugs. Among them are monoterpenes and sesquiterpenes, standard components of essential oils. This work evaluated the *in vitro* activity of monoterpenes, sesquiterpenes, and semi-synthetic derivatives against *Eisenia foetida* using albendazole as a positive control. Gas chromatography coupled with mass spectrometry was used to determine the structure of the derivatives. *In silico* analysis was also performed on probable molecular targets such as β -tubulin, acetylcholinesterase (AChE), and γ -aminobutyric acid B (GABA B) receptor. The compounds with hydroxyl groups in their structure, such as linalool and (*S*)-*cis*-verbenol, showed better biological activity, superior to the reference drug. The binding affinity of these compounds was also found *in silico* with AChE, GABA B receptor, and β -tubulin. These results demonstrate that natural products may constitute lead compounds for developing new anthelmintic drugs.

INTRODUCTION

According to data from the World Health Organization, soil-transmitted helminthiasis are among the leading causes of morbidity in developing countries [1]. These diseases mainly affect deprived sectors of the population. On the other hand, few drugs are available for treatment, and parasites developing resistance is a constant threat. [2]. Moreover, drugs in clinical use are not devoid of adverse effects [3]. As a result, there is a need to find new agents to combat infections by such pathogens in humans.

The chemistry of natural products is particularly interesting in this search because plants have been used since ancient times to treat various conditions and are sources of active molecules against numerous ailments. Essential oils are a

group of natural products known for their remarkable biological activities, including antitumor, antimicrobial, antiparasitic, and cardiovascular disease-fighting properties [4,5]. These oils are complex mixtures of volatile compounds extracted from aromatic plants, with monoterpenes and sesquiterpenes (and sometimes phenylpropanes) being the primary constituents responsible for their biological activities. However, there are few studies on the anthelmintic effects of these constituents and their semisynthetic derivatives. [6].

In this study, molecules that are components of essential oils such as (*R*)-limonene, (*S*)-limonene, (*S*)-*cis*-verbenol, linalool, *trans*-anethole, and caryophyllene oxide have been evaluated. Essential oils containing these compounds have demonstrated good antimicrobial and antiparasitic activities [7–12].

It is important to consider the relationship between the activity of compounds and their functional groups. Generally, oxygenated compounds in essential oils have stronger actions than hydrocarbons. Monoterpenes and sesquiterpenes with

*Corresponding Author

Nelson Luis Alvarenga, Phytochemistry Department, Faculty of Chemical Sciences, National University of Asunción, San Lorenzo, Paraguay.

E-mail: nelson@qui.una.py

†Contributed equally.

oxygenated functional groups are amphipathic due to their hydrocarbon moieties. Typically, the activity of essential oil components follows this order: phenols > aldehydes > ketones > alcohols > ethers > hydrocarbons, a trend observed against various bacteria and fungi [13]. It remains to be determined whether this trend is similar regarding anthelmintic activity. Therefore, in this work, the hydroxyl group of (*S*)-*cis*-verbenol and linalool were blocked as acetate to evaluate its implication in the activity assayed (Fig. 1).

In addition, it is crucial to evaluate the *in-silico* interactions of these molecules with potential cellular targets. One such target is β -tubulin, a cytoskeleton protein affected by several molecules, including albendazole, an anthelmintic drug. Combining *in vitro* tests with *in silico* interaction studies of candidate molecules with β -tubulin can identify compounds with similar activities to albendazole and other related anthelmintics. Other significant molecular targets include the acetylcholinesterase (AChE) and the γ -aminobutyric acid B (GABA B) receptor, as substances with anthelmintic activity have shown interactions with these targets, which are associated with helminth motility.

In addition to all the points mentioned above, there is a growing interest in the search for new molecules to combat these parasitic infections because they pose a significant public health problem in various countries. These infections lead to a high disease burden, severity, complications, and

morbidity, substantially impacting the population's health [14]. For all these reasons, this study has evaluated the compounds mentioned above to determine if they can be candidates for developing new anthelmintic drugs.

MATERIALS AND METHODS

Chemicals

(*R*)-(+)-limonene, (*S*)-(-)-limonene, linalool, (*S*)-*cis*-verbenol, *trans*-anethole, and (-)-caryophyllene oxide were purchased from Sigma-Aldrich.

Anthelmintic activity

The assay was performed with *Eisenia foetida*, commonly known as the Californian red worm. This helminth was chosen because of its anatomical and physiological similarities with human intestinal parasites and its ease of breeding and maintenance. The worms used in the *in vitro* study came from the Phytochemistry Department hatchery. The worms selected for the assay were 4 to 6 cm long and 0.2 to 0.4 cm wide.

The compounds at a 1 mg/ml concentration were dissolved in 5% dimethyl sulfoxide and saline solution to perform the assay. The positive control was albendazole, the drug most used clinically to treat helminthiasis in humans. The anthelmintic activity was performed according to Pawar's method, which consisted of placing three worms in a Petri dish and putting them in contact with the compounds to be tested and the controls. Subsequently, the time of paralysis and the time of death were recorded. The death time was confirmed by placing the worm in a container with water at 50°C, in which the worm should not show any movement or reincorporate. The assays were performed in triplicate [15].

Chemical modifications

Conventional chemical modifications were performed to obtain semi-synthetic derivatives. The modifications were intended to block the hydroxyl groups of the alcohols linalool and (*S*)-*cis*-verbenol as acetate esters.

Linalyl acetate preparation

504.8 mg of linalool was placed in a round-bottomed flask with 14 ml of acetic anhydride and 10 ml of pyridine with constant agitation at room temperature for ten days. The reaction was monitored every 24 hours by thin-layer chromatography using a mixture of hexane: ethyl acetate in a 9:1 ratio as the mobile phase. The reaction was completed with the addition of 30 ml of cold distilled water, and then liquid-liquid extraction was performed with 25 ml of chloroform. The extraction procedure was repeated four times. The organic phase was mixed with three portions of 25 ml of 10% HCl and separated again. Finally, the organic phases were combined, and anhydrous sodium sulfate was added to remove water, filtered with quantitative filter paper, and the solvent was eliminated with a rotary evaporator [16].

The purification was performed by column chromatography with silica gel as the stationary phase (Kieselgel 60 G) and a mixture of hexane: ethyl acetate (9:1) as the mobile phase.

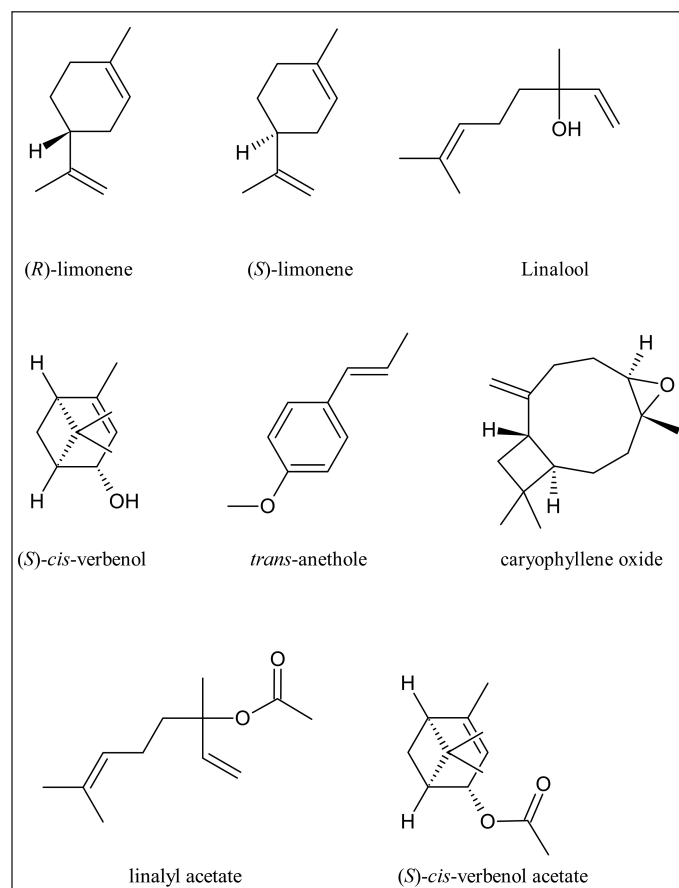


Figure 1. Structure of the mono and sesquiterpenes assayed.

(S)-*cis*-verbenol acetate preparation

536.2 mg of (*S*)-*cis*-verbenol was mixed with 14 ml of acetic anhydride and 10 ml of pyridine with constant stirring at 1,200 rpm at room temperature for approximately 5 hours and 45 minutes. As mentioned above, reaction monitoring was performed by thin-layer chromatography every 1 hour. The reaction was completed with the addition of 30 ml of cold distilled water, and then a liquid–liquid partition was carried out with 25 ml of chloroform. This procedure was repeated four times. The organic phase was mixed with three portions of 25 ml of 10% HCl and stirred in a separating funnel. Finally, the organic phase was separated, and anhydrous sodium sulfate was added to remove the remaining water from the organic solvent. As discussed earlier, it was filtered, and the solvent was eliminated in a rotary evaporator [16].

Purification was performed by column chromatography in the same conditions as mentioned before.

Gas chromatography-mass spectrometry determination of the semisynthetic derivatives

Solutions of the compounds were prepared at a concentration of 5 mg/ml in High-Performance Liquid Chromatography HPLC-grade acetonitrile (Merck KgaA, Darmstadt, Germany). Then, 1 μ l was injected into a Shimadzu QP-2010 Plus gas chromatograph (Shimadzu Corporation, Kyoto, Japan) under the following conditions: Rtx-5MS column (Restek, Bellefonte, PA) 30 m long, 0.25 mm diameter and 0.25 μ m thick stationary phase; Helium carrier gas (flow rate 1.3 ml/minutes), injection temperature 150°C, interface temperature 230°C, temperature gradient elution starting at 45°C and maintaining that temperature for 3 minutes and then increasing the temperature to 230°C at a rate of 5°C per minute and then maintaining the final temperature for 3 minutes. Electronic impact was used as the ionization technique at 70 eV in scanning mode (SCAN) with a scanning time of 0.5 seconds and a mass range from 60 to 600 Da. The compounds were identified by comparing the mass spectra obtained with those found in the NIST 107, VOL-FOOD, and NIST21 libraries.

Purity check of derivatives

The purity of the derivatives was verified by Nuclear Magnetic Resonance ¹H NMR spectroscopy (Spinsolve 60 NMR spectrometer, Magritek, Aachen, Germany). The corresponding spectra are provided in supplementary files 1 and 2.

In silico analysis

Selection of target proteins

The selection of target proteins was performed based on other studies [17–19]. These proteins were AChE (PDB: 4PQE), GABA B receptor (PDB: 4MS3), and β -tubulin (PDB: 1JFF), which are widely used in anthelmintic activities research [17–19].

Characterization of ligand binding sites on target proteins

Water and co-crystallized ligand molecules were removed from the target structures using Discovery Studio Visualizer v.20 (Dassault Systèmes, BIOVIA). Identification of

ligand binding sites and residues with probability of activity (>50%) in the target proteins (AChE, GABA B receptor, and β -tubulin) was performed by machine learning methods using GraSP software [20].

Molecular docking simulation assays

Docking simulations were performed with linalool and (*S*)-*cis*-verbenol because these compounds demonstrated important anthelmintic activities *in vitro*. Protein and compound structures were obtained from Protein Data Bank RCSB and PubChem databases [17–19,21,22]. Compound structures that were not found in the PubChem database were generated with ACD/ChemSketch 1.0 software [23].

The energetic minimization of structures was performed using Merck molecular force field (MMFF94) for small molecules, four steps per update with the conjugate gradient algorithm, a cycle of 50,000 steps, and energy convergence criteria of 0.001 kcal·mol⁻¹·Å⁻¹. We added partial charges and polar hydrogen atoms at a cell physiological pH of 7.4 with the Avogadro software [24].

Molecular docking simulations were performed using interaction boxes with dimensions of 63 × 71 × 54 Å³ for AChE, 87 × 80 × 71 Å³ for the GABA B receptor, and 61 × 59 × 61 Å³ for β -tubulin. These tests were performed with the program AutoDock Vina v.1 [25].

The dissociation constant (K_d) was determined employing equation 1 (Eq. 1), and ligand efficiency (LE) with equation 2 (Eq. 2); these equations were used by Choudhury and collaborators [26] and Onawole *et al.* (2018) [27], respectively:

$$K_d = e^{(\Delta G \times 1000 / RT)} \quad (1)$$

$$LE = -\Delta G / HA \quad (2)$$

where temperature (*T*) = 310 K (37°C), Ideal Gas Constant (*R*) = 1.987207 cal·mol⁻¹·K⁻¹, HA = the number of heavy atoms present in the chemical structure of the ligand.

These parameters give information about the affinity of compounds to the target protein and the efficiency of molecules as a possible effective drug candidate [26,27].

The Complexes were analyzed and visualized with Discovery Studio Visualizer v.20 software (Dassault Systèmes, BIOVIA).

Bioavailability predictions according to the modified Lipinski's rule of five (molecular weight ≤ 500 g·mol⁻¹, Moriguchi's water: octanol participation ratio ≤ 4.15, hydrogen bond acceptors ≤ 10, hydrogen bond donors ≤ 5) [28], as well as pharmacokinetic and toxic properties absorption, distribution, metabolism, excretion, and toxicity (ADME-Tox) of these compounds were performed with the SwissADME [29–31] and ProToxII tool [32].

RESULTS AND DISCUSSION

Anthelmintic activity against *E. foetida* of the unmodified compounds

The anthelmintic activity concerning the paralysis time of *E. foetida* is detailed in Figure 2.

The six compounds showed better paralysis time than the positive control (albendazole). The order of activity was as follows: linalool > (*S*)-*cis*-verbenol > caryophyllene oxide > (*S*)-(-)-limonene = (*R*)-(+)-limonene > *trans*-anethole. Linalool and (*S*)-*cis*-verbenol showed the better activity. This is consistent since both share a common characteristic: the hydroxyl group. These compounds showed lower paralysis times not only with albendazole but also with the other compounds tested. The common presence of hydroxyl suggests that this group has a great implication in the activity of these molecules against helminths. Except for this aspect, the differences between the two compounds are several: linalool is an acyclic monoterpene whose functional group is a tertiary alcohol, and (*S*)-*cis*-verbenol is a bicyclic monoterpene whose functional group is a secondary alcohol; therefore, they present an important structural and spatial difference. On the other hand, a statistically significant difference was observed when comparing the activity of both compounds between them, with linalool being more active.

As for (*S*)-(-)-limonene and (*R*)-(+)-limonene, both presented similar activity and did not show statistically significant differences between them. These compounds lack oxygen atoms; therefore, they present a lipophilic character, and the activity could be associated with this aspect, but the activity is not stereospecific since there is no difference between them. The last compound is *trans*-anethole, which, despite having oxygen in its structure, did not surpass the activity of the hydrocarbon compounds mentioned above. Because of this, it is inferred that the presence of oxygen alone does not confer significant activity, but the form in which it is found (alcohol, ether) and its location in the molecule is also relevant. *Trans*-anethole and caryophyllene oxide are ethers, but in the case of the latter, the ether is an oxacyclopropane, and these are very susceptible to opening due to attack by nucleophiles present in the medium.

Regarding the time of death, the results are observed in Figure 2, and the order of activity of compounds that caused helminth death is linalool > *cis*-verbenol > caryophyllene oxide

> *trans*-anethole. (*R*)-(+)-limonene and (*S*)-(-)-limonene did not cause helminth death.

Based on what has been observed so far, hydroxyl functional groups, or the presence of oxygen in the structure, play an important role in the lethal action.

The hydroxyl groups of linalool and (*S*)-*cis*-verbenol were blocked as esters to confirm this assertion.

Regarding linalyl acetate, 361.4 mg (71.6% yield) of the product was obtained.

Gas chromatography coupled with mass spectrometry was performed to verify that the desired product was obtained. The chromatogram in Figure 3 was obtained, and the mass spectrum is also shown. The identity of the compound was confirmed when compared with the equipment's databases. The purity of the compound was confirmed by ¹H NMR spectroscopy (Supplementary file 1).

Related to (*S*)-*cis*-verbenol acetate synthesis, 500.9 mg of the derivative was obtained, yielding 93.4%.

To confirm the product's identity, gas chromatography coupled with mass spectrometry was performed as in the previous case (Fig. 3). This identified the compound as (*S*)-*cis*-verbenol acetate, thus supporting the attainment of the desired compound. Purity was confirmed as above (Supplementary file 2).

Anthelmintic activity of the semi-synthetic derivatives

As shown, the derivatives showed better activity than albendazole, and the anthelmintic activity in terms of paralysis time presented the following range: (*S*)-*cis*-verbenol acetate > linalool acetate, showing significant differences between the compounds.

Regarding the time to death, it is highlighted that linalool acetate did not cause helminth death, so the hydroxyl group of the base structure is essential to producing death in this compound, as seen in Figure 4.

It is observed that upon acetylation of the hydroxyl group, both linalool and (*S*)-*cis*-verbenol decrease their activity considerably, and even concerning the time of death in the case

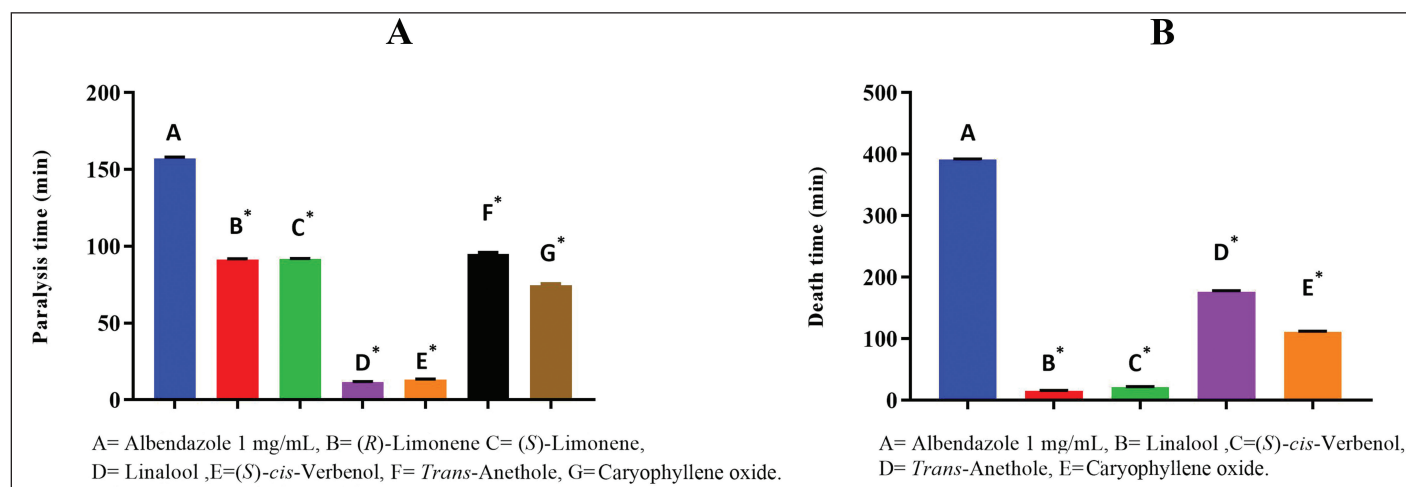


Figure 2. (A) Paralysis time and (B) death time of terpenes against *Eisenia foetida*, letters marked with an asterisk indicated statistically significant differences respect to control.

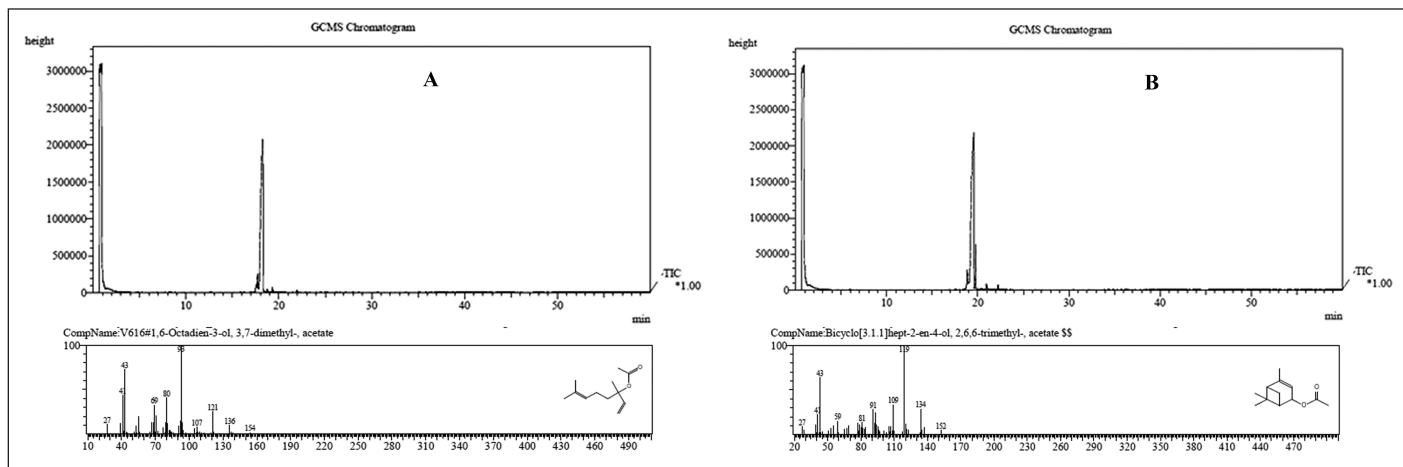


Figure 3. (A) Gas chromatogram and mass spectrum of linalyl acetate (A). (B) Gas chromatogram and mass spectrum of (*S*)-*cis*-verbenol acetate.

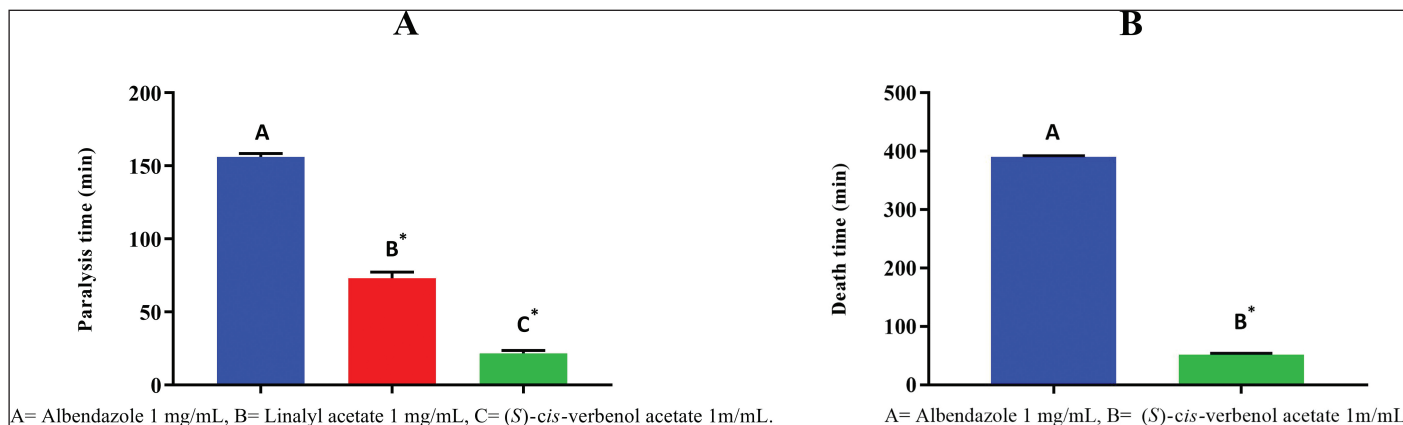


Figure 4. (A) Paralysis time and (B) death time of semisynthetic derivatives against *Eisenia foetida*. Letters marked with an asterisk indicate statistically significant differences with the control.

of linalool acetate involved the total loss of the activity of that compound, which highlights the importance of the hydroxyl group in this aspect.

In silico analysis

The structural analysis of the selected target proteins (AChE, GABA B Receptor, β -Tubulin) identified sites of probable interaction with ligands, which are observed in Figure 5.

The residues with the highest probability of activity were identified in the structure of AChE as Tyrosine (Tyr72), Tyr119, Glycine (Gly120), Gly121, Gly122, Tyr124, Glutamic Acid (Glu202), Serine (Ser203), Tryptophan Trp236, Trp286, Leucine (Leu289), Phenylalanine (Phe295), Arginine (Arg296), Phe297, Tyr337, Phe338, Tyr341, Histidine (His447), and Tyr449 (Fig. 5A). This site in the protein agrees with the location of the catalytic and its peripheral site reported in other investigations [33,34].

In the GABA B receptor structure, the active residues identified were Trp65 Cysteine (Cys103), Gly128, Cys129, Ser130, Ser131, Gly151, Ser152, Ser153, Ser154, Threonine (Thr159), Arg168, Thr169, Arg174, Thr175, Ser178, Thr202,

Ser231, Phe232, Phe319, Gly356, Tyr357, Aspartic Acid (Asp360), Thr412, Arg422 (Fig. 5B). As reported in a previous study, these residues formed part of the active site [35].

As for β -tubulin, the residues with the highest probability of interaction to ligands were Ala9, Gly10, Glutamine (Gln11), Cys12, Gly13, Asparagine (Asn14), Gln15, Valine (Val23), Asp26, Glu27, Ala99, Gly100, Asn101, Thr138, Ser140, Gly142, Gly143, Gly144, Thr145, Gly146, Ser147, Gly148, Asp179, Glu183, Tyr224, Asn228, His229, Leu230, Ala233, Ser236, Phe272, Proline (Pro274), Leu275, Thr276, Arg278, Pro360, Arg369, Gly370 (Fig. 5C). Also, this site agrees with the active site reported by Löwe *et al.* [36].

The molecular docking simulations performed with AChE showed that the compounds linalool (PubChem Compound Identification PubChem CID: 6549) and (*S*)-*cis*-verbenol (PubChem CID: 87839) presented similar free binding energy values ΔG of -5.8 and -5.6 kcal \cdot mol $^{-1}$, respectively. Thus, also the K_d values, which give quantitative information about binding affinities, were 81.41 and 112.64 μ M, respectively (Table 1). Regarding the estimation of LE, values of 0.53 and 0.51 were obtained, respectively; the optimal LE values are close to ≤ 0.3 . However, this strictly depends on the molecular

structure of compounds and the ΔG registered in complexes [37,27].

In the complex AChE: linalool, the hydrogen bond between linalool and Phe295 was registered. Also, alkyl interactions with Val294 and interactions between π orbitals of residues Tyr72, Trp286, Tyr124, Phe297, Phe338, Tyr341, and the alkyl regions of the compound, and Van der Waals interactions with residues of the pocket site were detected (Fig. 6A).

In the AchE:(*S*)-*cis*-verbenol complex, the registered interactions with the molecule were hydrogen bond with Arg296, alkyl interactions with Val294, interactions between alkyl chains (*S*)-*cis*-verbenol and π orbitals of residues Tyr341, Phe338, Tyr337, Trp286, and Van der Waals interactions with the binding site residues as observed in Figure 6B.

Simulation carried out with the structure of the GABA B receptor showed linalool and (*S*)-*cis*-verbenol demonstrate similar ΔG values of -5.0 and -5.7 kcal·mol⁻¹, respectively. The Kd values registered were 298.34 and 95.76 μ M, and the LE values were 0.45 and 0.52, respectively (Table 1).

The GABA B: linalool complex showed hydrogen bond with Arg243 and Asp459, alkyl interactions between the aliphatic chain of residues Ala242, Lys191, Ala193, and Van der Waals interactions with pocket site residues as observed in Figure 6C.

The GABA B:(*S*)-*cis*-verbenol complex showed a hydrogen bond with Arg207, interactions between the aliphatic region of the molecule and π orbitals of the residue chains Phe354, Trp284, Phe319, and Van der Waals interactions with residues of the pocket binding site (Fig. 6D).

Simulations between linalool and (*S*)-*cis*-verbenol to β -tubulin showed very similar ΔG values of -5.1 and -5.2 kcal·mol⁻¹, respectively. The Kd values were 253.63 and 215.63 μ M, and LE values of 0.46 and 0.47, respectively (Table 1).

In the β -tubulin: linalool complex, interactions detected were unconventional carbon hydrogen interactions between molecule and Ala233; this occurs between a polarized carbon next to an oxygen or nitrogen; the carbon acts as a hydrogen donor, so a weak hydrogen bond is generated [38]. Alkyl interactions were registered with Leu371 and Pro360, π -alkyl

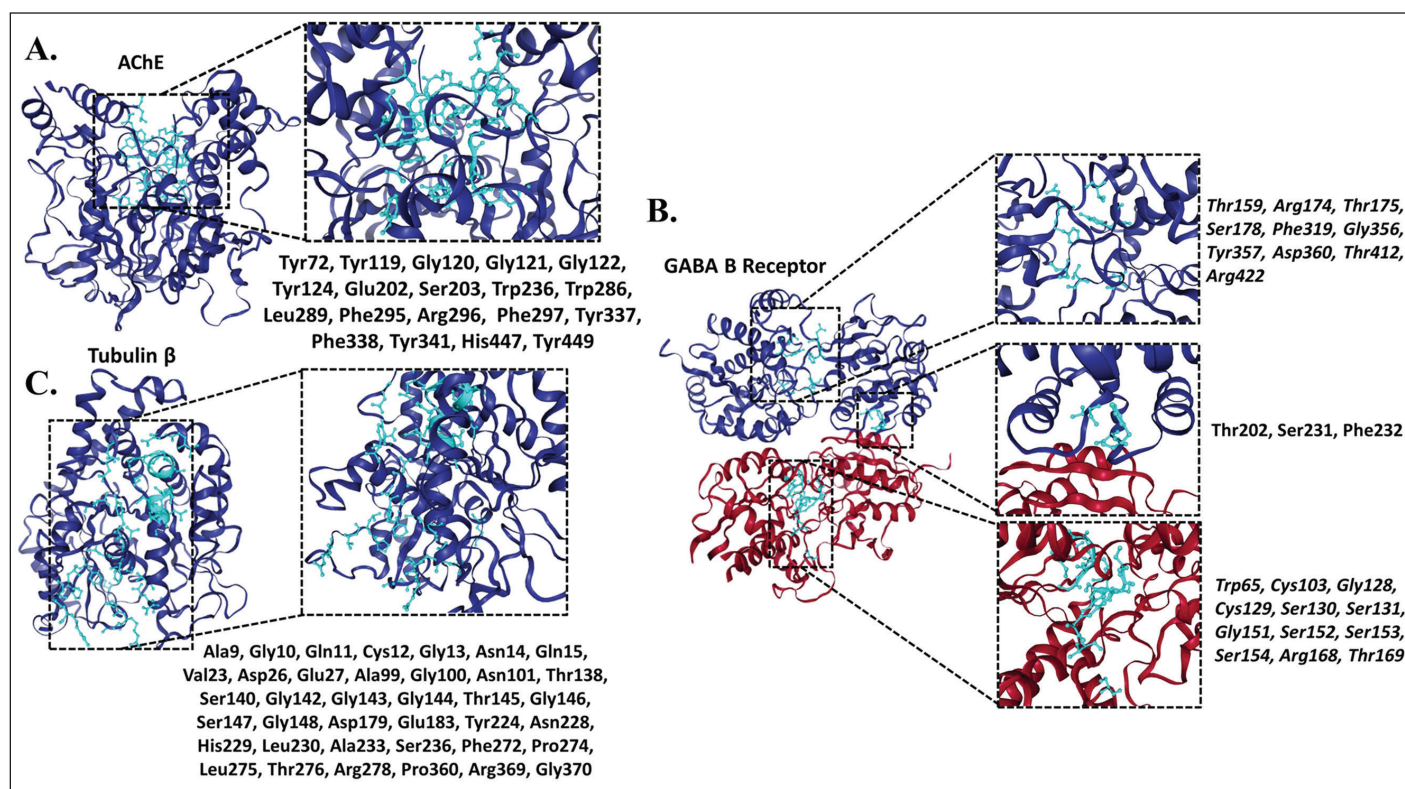


Figure 5. Ligand binding sites. (A) AChE, (B) GABA B receptor, red: chain A, blue: chain B, (C) β -tubulin.

Table 1. Molecular docking simulations results.

Compounds	ΔG (kcal·mol ⁻¹)			Kd (μ M)			LE		
	AChE	GABA B receptor	β -tubulin	AChE	GABA B receptor	β -tubulin	AChE	GABA B receptor	β -tubulin
Linalool	-5.8	-5.0	-5.1	81.41	298.34	253.63	0.53	0.45	0.46
(<i>S</i>)- <i>cis</i> -verbenol	-5.6	-5.7	-5.2	112.64	95.76	215.63	0.51	0.52	0.47

ΔG : binding free energy, Kd: dissociation constant, LE: ligand efficacy.

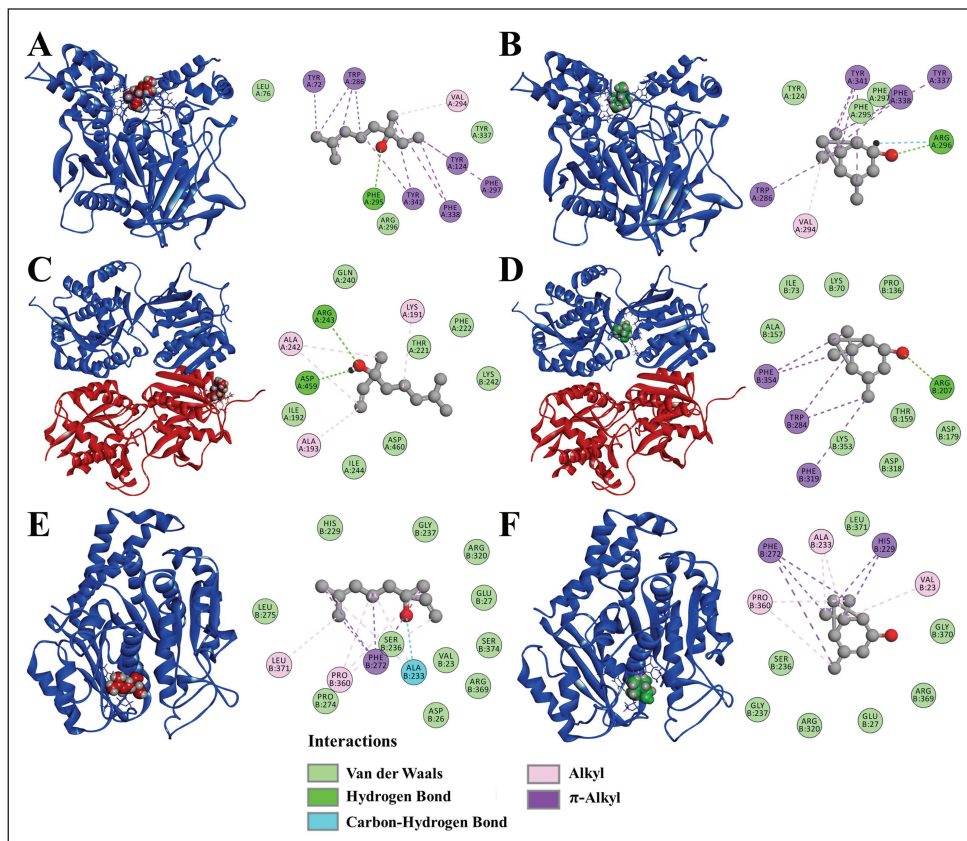


Figure 6. Three-dimensional and two-dimensional representations of complexes. (A) AChE:Linalool, (B) AChE:(*S*)-*cis*-verbenol, (C) GABA B:Linalool, red: Chain A, blue: Chain B, (D) GABA B:(*S*)-*cis*-verbenol, red: Chain A, blue: Chain B, (E) β -tubulin:Linalool, (F) β -tubulin:(*S*)-*cis*-verbenol.

interactions with Phe272, and Van der Waals interactions were also recorded with residues in the pocket binding site (Fig. 6E).

The β -tubulin: (*S*)-*cis*-verbenol complex revealed interactions between the alkyl chains of Pro360, Ala233, and Val23 and the molecule's aliphatic region. Also, π -alkyl interactions were detected with Phe272 and His229 residues, and Van der Waals interactions were detected with the binding site residues (Fig. 6F).

Many of these mentioned amino acids were previously reported as active residues and potential targets for ligand or inhibitor interaction in AChE protein, GABA B receptor, and β -tubulin (Fig. 5).

Hydrogen bonds are strong interactions associated with conformational distortion of ligands. They provide affinity energies between 0.25 and 40 kcal·mol⁻¹, approximately, and are one of the most critical interactions in the search for potential inhibitors [39].

Hydrophobic interactions are considered weak due to their low energetic contributions between 2 and 1.5 kcal·mol⁻¹. However, a correlation between compound binding affinities and the lipophilic surface of proteins has been reported because this interaction generates the rearrangement of water molecules in complexes, so it is mentioned that this interaction plays an essential role in the stability of the complex [39,40–42].

Interactions that involve π orbitals of residues or ligand compounds provide considerable molecular polarizations and

quadrupole moments, offering the ligand different molecular geometric options to adopt to establish structural stability. The existence of this type of interaction in complexes is desirable for the development of protein inhibitors [42].

Bioavailability predictions of the compounds according to the modified Lipinski's rule of five evidenced that all compounds evaluated in this study do not present violations of the rule (Table 2).

Regarding pharmacokinetic properties, it was observed that most of the compounds present high gastrointestinal absorption, except for *R*-limonene and *S*-limonene. Most of the compounds cannot inhibit any of the cytochrome P450 isoforms, except *R*-limonene and *S*-limonene, which could inhibit the Cytochrome P450 isoform 1A2 (CYP1A2) isoform, (-)-caryophyllene oxide which shows possible inhibition activity of Cytochrome P450 isoform 2C19 (CYP2C19), and Cytochrome P450 isoform 2C9 (CYP2C9) isoforms. Finally, *cis*-verbenol acetate showed evidence of CYP2C9 isoform inhibition (Table 3).

The prediction of toxicities showed that most of them do not present any activity except *trans*-anethole, which could have potential carcinogenic activities (Table 3).

The findings and *in vitro* activity suggest that the interaction with β -tubulin, AChE, and the GABA B receptor may not be the primary factors in the actions of linalool and (*S*)-*cis*-verbenol, despite being the most active. However,

Table 2. Prediction of oral bioavailability of compounds according to the modified Lipinski's rule.

Compounds	Molecular weight (g.mol ⁻¹)	H bond acceptors	H bond donors	MLOGP*	Violations
R-limonene	136.23	0	0	3.27	0
S-limonene	136.23	0	0	3.27	0
Linalool	154.25	1	1	2.59	0
(S)- <i>cis</i> -verbenol	152.23	1	1	2.3	0
<i>trans</i> -anethole	148.2	1	0	2.67	0
<i>trans</i> -caryophyllene	204.35	0	0	4.63	1
(-)-Caryophyllene oxide	220.35	1	0	3.67	0
Linalyl acetate	196.29	2	0	2.95	0
<i>cis</i> -verbenol acetate	194.27	2	0	2.65	0
Caryophyllene diepoxide	236.35	2	0	2.88	0

H: Hydrogen, *Moriguchi's octanol:water partition coefficient.

Table 3. Predictions of pharmacokinetic and toxic properties of compounds (ADME-Tox).

Compounds	GI	CYP450 inhibitors					Toxicity			
		CYP1A2	CYP2C19	CYP2C9	CYP2D6	CYP3A4	MUT	CAR	CYT	HEP
R-limonene	L	No	No	Yes	No	No	I	I	I	I
S-limonene	L	No	No	Yes	No	No	I	I	I	I
Linalool	H	No	No	No	No	No	I	I	I	I
(S)- <i>cis</i> -verbenol	H	No	No	No	No	No	I	I	I	I
<i>trans</i> -anethole	H	Yes	No	No	No	No	I	A	I	I
<i>trans</i> -caryophyllene	L	No	Yes	Yes	No	No	I	I	I	I
(-)-Caryophyllene oxide	H	No	Yes	Yes	No	No	I	I	I	I
Linalyl acetate	H	No	No	No	No	No	I	I	I	I
<i>cis</i> -verbenol acetate	H	No	No	Yes	No	No	I	I	I	I
Caryophyllene diepoxide	H	No	No	No	No	No	I	I	I	I

GI: Gastrointestinal absorption, L: Low, H: High, MUT: mutagenicity, CAR: Carcinogenesis, CYT: Cytotoxicity, HEP: Hepatotoxicity, I: Inactive, A: Active.

the binding energy values indicate that they may still have some involvement. Conversely, this may not be the case for (-)-caryophyllene oxide and *cis*-verbenol acetate, as these targets seem relevant for their actions. Further research is required to obtain precise data on the molecular-level mechanism of action of these compounds.

CONCLUSION

The compounds (*S*)-*cis*-verbenol and linalool showed outstanding anthelmintic activity against *E. foetida*. Considering their structure, the presence of the hydroxyl group in the chemical scaffold is crucial for their biological activity. Furthermore, they exhibited superior activity compared to the reference drug, suggesting that these compounds are promising candidates for further development as potential anthelmintic drugs.

Regarding the synthetic derivatives obtained, such as linalool acetate and (*S*)-*cis*-verbenol acetate, it was observed that blocking the hydroxyl group results in the partial loss of anthelmintic activity and, in the case of linalool, the loss of its lethal action. Therefore, the importance of the hydroxyl group is also established by performing the structure-activity analysis.

Concerning the *in silico* analysis, the two more active compounds showed potential binding affinity to the proteins tested, suggesting that they could be at least partially involved in their mechanism of action. However, further studies are required to elucidate and obtain more information about other possible targets for the anthelmintic action observed.

LIST OF ABBREVIATIONS

ΔG : gibbs free binding energy; AChE: acetylcholinesterase enzyme; ADME-Tox: absorption, distribution, metabolism, excretion and toxicity; Ala: alanine; Arg: arginine; Asn: asparagine; Asp: aspartic acid; CID: PubChem compound identification; CYP1A2: cytochrome P450 isoform 1A2; CYP2C19: cytochrome P450 isoform 2C19; CYP2C9: cytochrome P450 isoform 2C9; Cys: cysteine; GABA B: γ -aminobutyric acid B receptor; Gln: glutamine; Glu: glutamic acid; Gly: glycine; HA: number of heavy atoms; His: histidine; K: kelvin; Kd: dissociation constant; LE: ligand efficiency; Leu: leucine; MMFF94: merck molecular force field; NMR: nuclear magnetic resonance; PDB: protein data bank; Phe: phenylalanine; Pro: proline; R: ideal gas constant;

Ser: serine; T: temperature; Thr: threonine; Trp: tryptophan; Tyr: tyrosine; Val: valine.

AUTHOR CONTRIBUTIONS

All authors made substantial contributions to conception and design, acquisition of data, or analysis and interpretation of data; took part in drafting the article or revising it critically for important intellectual content; agreed to submit to the current journal; gave final approval of the version to be published; and agree to be accountable for all aspects of the work. All the authors are eligible to be an author as per the international committee of medical journal editors (ICMJE) requirements/guidelines.

FUNDING

There is no funding to report.

CONFLICTS OF INTEREST

The authors report no financial or any other conflicts of interest in this work.

ETHICAL APPROVALS

This study does not involve experiments on animals or human subjects.

DATA AVAILABILITY

All the data is available with the authors and shall be provided upon request.

PUBLISHER'S NOTE

All claims expressed in this article are solely those of the authors and do not necessarily represent those of the publisher, the editors and the reviewers. This journal remains neutral with regard to jurisdictional claims in published institutional affiliation.

USE OF ARTIFICIAL INTELLIGENCE (AI)-ASSISTED TECHNOLOGY

The authors declares that they have not used artificial intelligence (AI)-tools for writing and editing of the manuscript, and no images were manipulated using AI.

REFERENCES

- World Health Organization. The Top 10 Causes of Death [Internet]. 2018 [cited 2019 Mar 23]. Available from: <https://www.who.int/es/news-room/fact-sheets/detail/the-top-10-causes-of-death>
- Sangster N, Batterham P, Chapman HD, Duraisingh M, Le Jambre L, Shirley M, *et al.* Resistance to antiparasitic drugs: the role of molecular diagnosis. *Int J Parasitol.* 2002;32(5):637–53. doi: [http://doi.org/10.1016/s0020-7519\(01\)00365-4](http://doi.org/10.1016/s0020-7519(01)00365-4)
- Narciso-Schiavon JL, Delziovo HA, Santos LEB, Shiozawa MBC, Schiavon LL. Recurrent albendazole-induced acute hepatitis. *Rev Colomb Gastroenterol.* 2018;33(4):473–7. doi: <https://doi.org/10.22516/25007440.206>
- Edris AE. Pharmaceutical and therapeutic potentials of essential oils and their individual volatile constituents: a review. *Phytother Res.* 2007;323(1):308–23. doi: <http://doi.org/10.1002/ptr.2072>
- Yaluff G, Vega C, Alvarenga N. *In vitro* antiprotozoal activity of (S)-*cis*-Verbenol against *Leishmania* spp. and *Trypanosoma cruzi*. *Acta Trop.* 2017;168(1):41–4.
- Pérez C, Torres CNM. Antimicrobial activity and chemical composition of essential oils from verbenaceae species growing in. *Molecules.* 2018;23(3):544.
- Aelenei P, Rimbu CM, Guguianu E, Dimitriu G, Aprotosoae AC, Brebu M, *et al.* Coriander essential oil and linalool—interactions with antibiotics against Gram-positive and Gram-negative bacteria. *Lett Appl Microbiol.* 2018;68(2):156–64. doi: <http://doi.org/10.1111/lam.13100>
- Leite N, Sobral-Souza C, Albuquerque R, Brito Dara I, Lavor A, Alencar L *et al.* Actividad citotóxica y antiparasitaria *in vitro* del cariofileno y eugenol contra *Trypanosoma cruzi* y *Leishmania brasiliensis*. *Rev Cubana Plant Med [online].* 2013;18(4):522–8.
- Bano S, Intisar A, Rauf M, Ghaffar A, Yasmeen F, Zaman W, *et al.* Comparative analysis of oil composition and antibacterial activity of aerial parts of *Terminalia arjuna* (Roxb). *Nat Prod Res.* 2019;0(0):1–4. doi: <http://doi.org/10.1080/14786419.2018.1557656>
- Rahman A, Al-Reza S, Sattar M, Kang S. Potential roles of essential oil and extracts of *Piper chaba* Hunter to Inhibit *Listeria monocytogenes*. *Rec Nat Prod.* 2011;5(3):228–37.
- Taylor P, Asili J, Emami S, Eynolghozat R, Noghab Z. Chemical composition and *in vitro* efficacy of essential oil of seven *Artemisia* species against ESBL producing multidrug-resistant *Escherichia coli*. *J Essent Oil-Bear Plants.* 2015;18(1):124–45. doi: <http://doi.org/10.1080/0972060X.2014.895181>
- Xing C, Qin C, Li X, Zhang F, Linhardt RJ, Sun P, *et al.* Chemical composition and biological activities of essential oil isolated by HS-SPME and UAHF from fruits of bergamot. *LWT - Food Sci Technol.* 2019;104(1):38–44. doi: <https://doi.org/10.1016/j.lwt.2019.01.020>
- Kalemba D, Kunicka A. Antibacterial and antifungal properties of essential oils. *Curr Med Chem.* 2003 May;10(10):813–29. doi: <http://doi.org/10.2174/0929867033457719>
- Organización Mundial de la Salud. Estrategia de la OMS sobre medicina tradicional 2014–2023 [Internet]. 2013. Available from: <http://apps.who.int/medicinedocs/documents/s21201es/s21201es.pdf>
- Pawar SD, Patil YB, Premchandani LA, Borse SL, Borse LB, Pawar SP. Study of anthelmintic activity of chloroform extract of *Tinospora cordifolia*. *World J Pharm Pharm Sci.* 2014;3(6):2253–68. Available in: http://www.wjpps.com/wjpps_controller/abstract_id/1551
- Novato T, Gomes GA, Zeringóta V, Franco CT, de Oliveira DR, Melo D, *et al.* *In vitro* assessment of the acaricidal activity of carvacrol, thymol, eugenol and their acetylated derivatives on *Rhipicephalus microplus* (Acari: Ixodidae). *Vet Parasitol.* 2018;260:1–4. doi: <http://doi.org/10.1016/j.vetpar.2018.07.009>
- He F, Liu R, Tian G, Qi Y, Wang T. Ecotoxicological evaluation of oxidative stress-mediated neurotoxic effects, genetic toxicity, behavioral disorders, and the corresponding mechanisms induced by fluorene-contaminated soil targeted to earthworm (*Eisenia fetida*) brain. *Sci Total Environ.* 2023;871:162014. <http://doi.org/10.1016/j.scitotenv.2023.162014>
- Choudhary N, Khatik GL, Choudhary S, Singh G, Sutte A. *In vitro* anthelmintic activity of *Chenopodium album* and *in-silico* prediction of mechanistic role on *Eisenia fetida*. *Heliyon.* 2021;7(1):e05917. doi: <http://doi.org/10.1016/j.heliyon.2021.e05917>
- Mowla TE, Zahan S, Sami SA, Uddin SN, Rahman M. Potential effects and relevant lead compounds of *Vigna mungo* (L.) Hepper seeds against bacterial infection, helminthiasis, thrombosis and neuropharmacological disorders. *Saudi J Biol Sci.* 2022;29(5):3791–3805. doi: <http://doi.org/10.1016/j.sjbs.2022.03.008>
- Santana CA, Silveira SDA, Moraes JP, Izidoro SC, de Melo-Minardi RC, Ribeiro AJ, *et al.* GRaSP: a graph-based residue neighborhood strategy to predict binding sites. *Bioinformatics.* 2020;36(26):i726–i734. doi: <http://doi.org/10.1093/nar/gkac323>
- Berman HM, Westbrook J, Feng Z, Gilliland G, Bhat TN, Weissig H, *et al.* The protein data bank. *Nucl Acids Res.* 2020;28(1):235–242. doi: <http://doi.org/10.1093/nar/28.1.235>

22. Kim S, Chen J, Cheng T, Gindulyte A, He J, He S, *et al.* PubChem 2023 update. *Nucl Acids Res.* 2023;51(D1):D1373–D1380. doi: <http://doi.org/10.1093/nar/gkac956>
23. Hunter AD. ACD/ChemSketch 1.0 (freeware); ACD/ChemSketch 2.0 and its tautomers, dictionary, and 3D plug-ins; ACD/HNMR 2.0; ACD/CNMR 2.0. 1997. doi: <http://doi.org/10.1021/ed074p905>
24. Hanwell MD, Curtis DE, Lonie DC, Vandermeersch T, Zurek E, Hutchison GR. Avogadro: an advanced semantic chemical editor, visualization, and analysis platform. *J Cheminf.* 2012;4:17. doi: <http://doi.org/10.1186/1758-2946-4-17>
25. Trott O, Olson AJ. AutoDock vina: improving the speed and accuracy of docking with a new scoring function, efficient optimization, and multithreading. *J Comput Chem.* 2009;31(2):455–461. <http://doi.org/10.1002/jcc.21334>
26. Choudhury A, Das NC, Patra R, Bhattacharya M, Ghosh P, Patra BC, *et al.* Exploring the binding efficacy of ivermectin against the key proteins of SARS-CoV-2 pathogenesis: an *in silico* approach. *Future Virol.* 2021;16(4):277–291. <http://doi.org/10.2217/fvl-2020-0342>
27. Onawole AT, Kolapo TU, Sulaiman KO, Adegoke RO. Structure based virtual screening of the Ebola virus trimeric glycoprotein using consensus scoring. *Comput Biol Chem.* 2018;72:170–180. doi: <http://doi.org/10.1016/j.compbiolchem.2017.11.006>
28. Lipinski CA, Lombardo F, Dominy BW, Feeney PJ. Experimental and computational approaches to estimate solubility and permeability in drug discovery and development settings. *Adv Drug Deliv Rev.* 2012;64:4–17. <http://doi.org/10.1016/j.addr.2012.09.019>
29. Daina A, Michielin O, Zoete V. iLOGP: A simple, robust, and efficient description of n-octanol/water partition coefficient for drug design using the GB/SA approach. *J Chem Inf Model.* 2014;54(12):3284–3301. doi: <http://doi.org/10.1021/ci500467k>
30. Daina A, Zoete V. A BOILED-egg to predict gastrointestinal absorption and brain penetration of small molecules. *Chem Med Chem.* 2016;11(11):1117–1121.
31. Daina A, Michielin O, Zoete V. SwissADME: a free web tool to evaluate pharmacokinetics, drug-likeness and medicinal chemistry friendliness of small molecules. *Sci Reps.* 2017;7(1):42717. doi: <http://doi.org/10.1038/srep42717>
32. Banerjee P, Eckert AO, Schrey AK, Preissner R. ProTox-II: a webserver for the prediction of toxicity of chemicals. *Nucleic Acids Res.* 2018;46(W1):W257–W263. <http://doi.org/10.1093/nar/gky318>
33. Silman I, Sussman JL. Acetylcholinesterase: How is structure related to function? *Chem Biol Interact.* 2008;175(1–3):3–10. <http://doi.org/10.1016/j.cbi.2008.05.035>
34. Dvir H, Silman I, Harel M, Rosenberry TL, Sussman JL. Acetylcholinesterase: from 3D structure to function. *Chem Biol Interact.* 2010;187(1–3):10–22.
35. Geng Y, Bush M, Mosyak L, Wang F, Fan QR. Structural mechanism of ligand activation in human GABA B receptor. *Nature.* 2013;504(7479):254–259. <http://doi.org/10.1038/nature12725>
36. Löwe J, Li H, Downing KH, Nogales E. Refined structure of α -tubulin at 3.5 Å resolution. *J Mol Biol.* 2001;313(5):1045–1057. doi: <http://doi.org/10.1006/jmbi.2001.5077>
37. Hopkins AL, Keserü GM, Leeson PD, Rees DC, Reynolds CH. The role of ligand efficiency metrics in drug discovery. *Nat Rev Drug Discov.* 2014;13(2):105–121. <http://doi.org/10.1038/nrd4163>
38. Gómez-Jeria JS, Robles-Navarro A, Kpotin GA, Garrido-Sáez N, Gatica-Díaz N. Some remarks about the relationships between the common skeleton concept within the Klopman-Peradejordi-Gómez QSAR method and the weak molecule-site interactions. *Chem Res J.* 2020;5(2):32–52. Available from: <https://chemrj.org/archive/volume-5-issue-2-2020/>
39. Zhou P, Huang J, Tian F. Specific noncovalent interactions at protein-ligand interface: implications for rational drug design. *Curr Med Chem.* 2012;19(2):226–238.
40. Patil R, Das S, Stanley A, Yadav L, Sudhakar A, Varma AK. Optimized hydrophobic interactions and hydrogen bonding at the target-ligand interface leads the pathways of drug-designing. *PLoS ONE.* 2010;5(8):e12029.
41. Böhm HJ, Klebe G. What can we learn from molecular recognition in protein–ligand complexes for the design of new drugs? *Angew Chem Int Ed Engl.* 1996;35(22):2588–2614. doi: 10.1002/anie.199625881
42. Bissantz C, Kuhn B, Stahl M. A medicinal chemist’s guide to molecular interactions. *J Med Chem.* 2010;53(14):5061–5084. doi: <https://doi.org/10.1021/jm100112j>

How to cite this article:

Cáceres AL, Gayoso E, Guillen R, Alvarenga NL. *In vitro* anthelmintic activity and *in silico* analysis of monoterpenes, sesquiterpenes, and semisynthetic derivatives against *Eisenia foetida*. *J Appl Pharm Sci.* 2025;15(01):196–205.

SUPPLEMENTARY MATERIAL

The supplementary material can be accessed at the journal's website: link here [https://japsonline.com/admin/php/uploadss/4408_pdf.pdf].